Unbound states of ^{32}Cl and the ^{31}S(p,γ)^{32}Cl reaction rate

M. Matoš, J. C. Blackmon, L. E. Linhardt, D. W. Bardayan, C. D. Nesaraja, J. A. Clark, C. M. Deibel, P. D. O'Malley, and P. D. Parker

Unbound states of ^{32}Cl and the ^{31}S$(p,\gamma)^{32}$Cl reaction rate

M. Matoš,* J. C. Blackmon, and L. E. Linhardt

Department of Physics & Astronomy, Louisiana State University, Baton Rouge, LA 70803, USA

D. W. Bardayan and C. D. Nesaraja

Physics Division, Oak Ridge National Laboratory, Oak Ridge, TN 37831, USA

J. A. Clark

Physics Division, Argonne National Laboratory, Argonne, IL 60439, USA

C. M. Deibel

Physics Division, Argonne National Laboratory, Argonne, IL 60439, USA and

Joint Institute for Nuclear Astrophysics, Michigan State University, East Lansing, MI 48824, USA

P. D. O'Malley

Department of Physics and Astronomy, Rutgers University, Piscataway, NJ 08854, USA

P. D. Parker

Wright Nuclear Structure Laboratory, Yale University, New Haven, CT 06520, USA

(Dated: November 9, 2011)

The ^{31}S$(p,\gamma)^{32}$Cl reaction is expected to provide the dominant break-out path from the SiP cycle in novae and is important for understanding enrichments of sulfur observed in some nova ejecta. We studied the ^{32}S(^{3}He,t)^{32}Cl charge-exchange reaction to determine properties of proton-unbound levels in ^{32}Cl that have previously contributed significant uncertainties to the ^{31}S$(p,\gamma)^{32}$Cl reaction rate. Measured triton magnetic rigidities were used to determine excitation energies in ^{32}Cl. Proton-branching ratios were obtained by detecting decay protons from unbound ^{32}Cl states in coincidence with tritons. An improved ^{31}S$(p,\gamma)^{32}$Cl reaction rate was calculated including robust statistical and systematic uncertainties.

PACS numbers: 25.40.Lw, 26.30.Ca, 26.50.+x, 27.30.+t

* E-mail: matos@lsu.edu

I. INTRODUCTION

A classical nova is a cataclysmic nuclear explosion on the surface of a white dwarf star resulting from the accretion of hydrogen-rich gas from a companion star. A sequence of nuclear reactions produces a sudden luminosity increase by up to a factor of a million and ejects matter from the white dwarf. The time scales of explosive hydrogen burning processes are influenced by the duration of reaction cycles closed by (p,α) reactions, with break out via (p,γ) reactions competing with β-decays. The SiP cycle is one such cycle, which is of particular interest for understanding novae like Nova Her 1991 that are observed to exhibit high sulfur abundances compared to solar values [1, 2].

In the SiP cycle the ^{31}S$(p,\gamma)^{32}$Cl reaction is believed to be the dominant break-out reaction [3]. The rate of the ^{31}S$(p,\gamma)^{32}$Cl reaction at nova temperatures is dominated by resonances corresponding to states in the compound nucleus ^{32}Cl. The ^{31}S$(p,\gamma)^{32}$Cl reaction rate was previously calculated based on some measured resonance properties and estimates of others based upon the mirror nucleus ^{32}P [4]. Uncertainties in the rate were provided in a subsequent reanalysis [5]. The ^{32}Cl excitation energies near the proton threshold of $Q_p = 1581.3(6)$ keV [6] used by Ref. [4, 5] were based on earlier measurements that disagreed at the 2 sigma level (by 10-20 keV) [3, 7], and the resonance strengths were only constrained based upon properties of states in the mirror. A recent study of 5 states below 2.3 MeV via the ^{32}S$(^{3}$He,$t)^{32}$Cl reaction [8] is in agreement with the excitation energies reported by Ref. [3]. However, significant uncertainties remain regarding resonance strengths and size of systematic uncertainties in the resonance energies.

We have studied proton-unbound states in ^{32}Cl using the ^{32}S$(^{3}$He,$t)^{32}$Cl charge-exchange reaction. Excitation energies and proton-branching ratios for states of astrophysical interest for the ^{31}S$(p,\gamma)^{32}$Cl reaction rate were determined. In the following sections we describe the experiment and new results for states in ^{32}Cl, including the observation of a predicted, but previously unobserved, level. We then present calculations of a new recommended ^{31}S$(p,\gamma)^{32}$Cl reaction rate based on these new results including statistical and systematic uncertainties.

II. EXPERIMENT

We used the charge-exchange reaction ^{32}S$(^{3}$He,$t)^{32}$Cl to populate states in ^{32}Cl. A 30-MeV ^{3}He^{2+} beam from the Extended Stretched TransUranium (ESTU) tandem Van de Graaff accelerator at the Wright Nuclear Structure Laboratory (WNSL) at Yale University bombarded ZnS targets. Targets with thicknesses of 240 μg/cm^2 and 350 μg/cm^2 both on 5 μg/cm^2 carbon substrates were produced via evaporation at Oak Ridge National Laboratory and used in the experiment at the WNSL. Their thicknesses were determined with about 10% uncertainty via energy loss
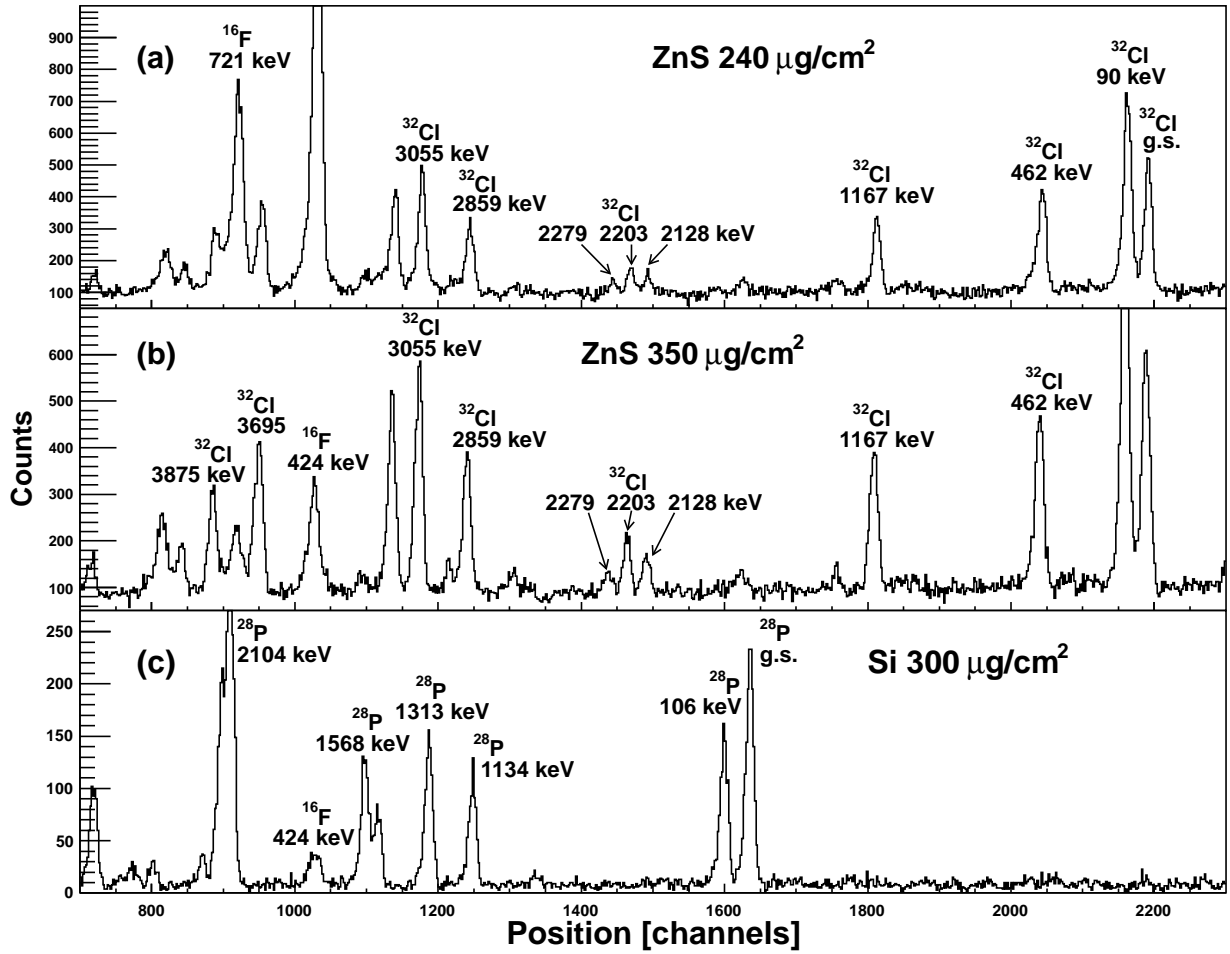
FIG. 1. Spectra showing position of tritons at the focal plane measured by the ionization chamber with the Enge spectrograph set at 3°. Three spectra show results from measurements with three targets, 240 μg/cm^2 ZnS, 350 μg/cm^2 ZnS and a 300 μg/cm^2 Si target. Peaks are identified with the final level in the nucleus produced.

measurements of α particles from a ^{241}Am source. A 150 μg/cm^2 CdS target on a 20 μg/cm^2 substrate was used at one angle (5°) but had worse energy resolution and lower counting rates and was therefore not used at other angles. Additional data were taken with a 300 μg/cm^2 natural Si target for calibration and a 900 μg/cm^2 Zn target for background analysis.

Reaction products were separated and analyzed with the Enge split-pole spectrograph at the WNSL. The spectrograph separates particles according to their magnetic rigidities, $B\rho$, so that discrete positions at the focal plane correspond to discrete momenta. The positions of detected particles at an Enge focal plane were determined by a position-sensitive ionization drift chamber filled with 150 Torr of isobutane gas [9]. As the ions pass through the gas, the amount of charge collected by the cathode determines the energy lost in the detector. The residual energy

was measured by a thick plastic scintillator located behind the ionization chamber. Measurements were conducted at spectrograph (laboratory) angles of 3°, 5°, 10° and 20°. At the 3° setting the protons emitted from excited states in ^{32}Cl were detected in coincidence with outgoing tritons by the Yale Lamp Shade Array (YLSA) [10] consisting of four 16-strip silicon detectors arranged in a lamp-shade configuration. The YLSA detectors covered an angular range of $\theta_{lab} = 131°$ to $\theta_{lab} = 166°$ and were calibrated with α particles from a ^{241}Am source.

III. LEVEL ENERGIES

Tritons were identified at the focal plane of the spectrograph using the E_{res} vs. ΔE relationship from the ionization chamber and the scintillator. Focal-plane position spectra gated on tritons are shown in Fig. 1, and states in ^{32}Cl populated via the ^{32}S(^{3}He,t)^{32}Cl charge-exchange reaction are labeled. Tritons corresponding to states in ^{16}F resulting from the ^{16}O(^{3}He,t)^{16}F reaction due to oxygen contamination in the targets are also seen in Fig. 1.

Positions at the focal plane were calibrated using known states in ^{28}P populated from the ^{28}Si(^{3}He,t)^{28}P reaction on a silicon target. The 424 keV ^{16}F state populated from oxygen contaminants in the targets, and the ground and 90 keV first excited states in ^{32}Cl were also used to calibrate the position spectra, providing 14 calibration points spanning the region of interest. Centroids were obtained by fitting a Gaussian function to each peak with a linear background, and the centroids of the calibration peaks were fit by their magnetic rigidities. Both 2nd and 3rd order polynomial functions were fit. Excitation energies for all states of astrophysical interest agreed within 1 keV from both fits, but the 3rd order fit function was adopted as it provided a better fit to the lowest and highest energy calibration peaks. The magnetic rigidities of the recoiling tritons were calculated from the reaction kinematics with the newest atomic mass values implemented [11, 12], including new values for ^{28}P and ^{32}Cl obtained recently, with mass excess of $-7147.5(12)$ keV, $-13333.8(12)$ keV, respectively [13]. Small corrections (<30 keV) were made for the energy loss of the incident ^{3}He ions and recoiling tritons in the target using the energy loss code STOPIT [14], assuming the reaction happened in the center of the target. The fit function was then used to obtain magnetic rigidities from the centroids for the peaks of interest. The energies of the levels were calculated from reaction kinematics taking energy losses into account. The statistical uncertainty in the energy of each state, ΔE_i, was calculated as a combination of the uncertainties originating from the centroid determination and the fitting function uncertainties estimated from covariance analysis. The energy resolution for each triton peak was typically about 40 keV (FWHM), and no peaks wider than the instrumental resolution were observed.

Excitation energies were obtained for each level at several angles and with the different targets. The final weighted

average for each state was calculated from these energies. The uncertainty in the excitation energy was assigned as the larger of the average uncertainty

$$\Delta E_{av} = \sqrt{\frac{1}{\sum_{i=1}^{n} \frac{1}{(\Delta E_i)^2}}} \tag{1}$$

and the scatter uncertainty

$$\Delta E_{scat} = \sqrt{\frac{1}{n-1} \frac{\sum_{i=1}^{n} \frac{(E - E_i)^2}{(\Delta E_i)^2}}{\sum_{i=1}^{n} \frac{1}{(\Delta E_i)^2}}}. \tag{2}$$

Systematic uncertainties were estimated using a Monte Carlo simulation, where the target thicknesses and mass values were randomly varied with Gaussian distribution probabilities. Mass and thickness uncertainties were used as standard deviations, σ. The systematic error was determined as the standard deviation of the Gaussian fit for the level energy distributions obtained in the Monte Carlo simulation. The systematic uncertainty was found to be 4 keV for all states, except for the 462 keV and 1167 keV states, where the systematic uncertainty was determined to be 2 keV and 3 keV, respectively.

The excitation energies determined from this measurement with statistical uncertainties are given in Table I. They are compared with other measurements [3, 7, 8] and the evaluation by [15]. The evaluation favored [3] over [7], where results from both measurements were available and generally adds 11 keV to [7] if only this one is available. The level energies determined in ^{32}Ar(β^+p) experiments include 461.1(1) keV, 1168.5(2) keV, and 4076(10) keV from [16] and 4072(9) keV from [17], all agreeing well with our results. A recent measurement also using the ^{32}S(^{3}He,t)^{32}Cl reaction provides energies for five levels between 1.3 and 2.3 MeV that are systematically higher than the current work by about 4 keV [8].

We have also discovered an excited state in ^{32}Cl at 2611(5) keV, shown in Fig. 2. The measured excitation energy for the new state is in good agreement with a 1^+ state predicted at 2574(50) keV based on the mirror nucleus ^{32}P and estimated using the IMME equation [4].

IV. PROTON UNBOUND STATES

The YLSA silicon-detector array was installed covering backward angles at the target position to measure decays of proton-unbound states in ^{32}Cl in coincidence with tritons detected with the spectrograph at $\theta_{lab} = 3°$. Figure 3 shows the energy of the protons detected by YLSA versus the position (corresponding to momentum) of the tritons at

the focal plane. A gate is shown around events corresponding to the proton decay of ^{32}Cl* to the ground state of ^{31}S ($J^\pi = 1/2^+$). Proton decay to excited states of ^{31}S was not possible for ^{32}Cl excited states below 2.8 MeV due to the ^{32}Cl proton-separation energy of $Q_p = 1581.3(6)$ keV [6] and the first excited state in ^{31}S being at 1248.9(2) keV [18].

TABLE I. Excitation energies in ^{32}Cl measured in this work compared to other measurements and evaluations. All listed uncertainties are statistical. Systematic uncertainties have been estimated in this work as 4 keV for all states, except for the 462 keV state with the systematic uncertainty of 2 keV and the 1167 keV state with the systematic uncertainty of 3 keV.

| this work [keV]	Jeanperrin [7] [keV]	Vouzoukas [3] [keV]	Endt [15] [keV]	Wrede [8] [keV]
462.0(10)	447(7)		461.1(1)	
1167.0(21)	1157(5)		1168.5(2)	
1327.4(29)	1326(5)	1329(3)	1331(3)	1331.2(5)
1734.2(14)	1719(4)	1735(3)	1733(2)	1736.7(6)
2127.5(19)	2122(5)	2129(3)	2130(3)	2131.1(4)
2203.1(28)	2193(7)	2213(3)	2212(3)	2209.5(5)
2278.6(25)	2270(5)	2281(3)	2281(3)	2283.5(5)
2610.9(30)				
2677.0(16)	2665(10)		2676(10)	
2859.2(14)	2858(5)		2869(5)	
2931.5(17)	2941(5)		2952(5)	
3054.7(14)	3056(5)		3067(5)	
3163.9(11)	3166(5)		3177(5)	
3280.8(23)	3290(10)		3301(10)	
3695.0(9)	3692(7)		3703(7)	
3874.8(17)	3883(5)		3894(5)	
3999.5(12)	4002(6)		4013(6)	
4073.6(11)	4080(7)		4074(7)	
4349.9(23)	4356(7)		4367(7)	
4577.1(30)	4590(8)		4601(8)	
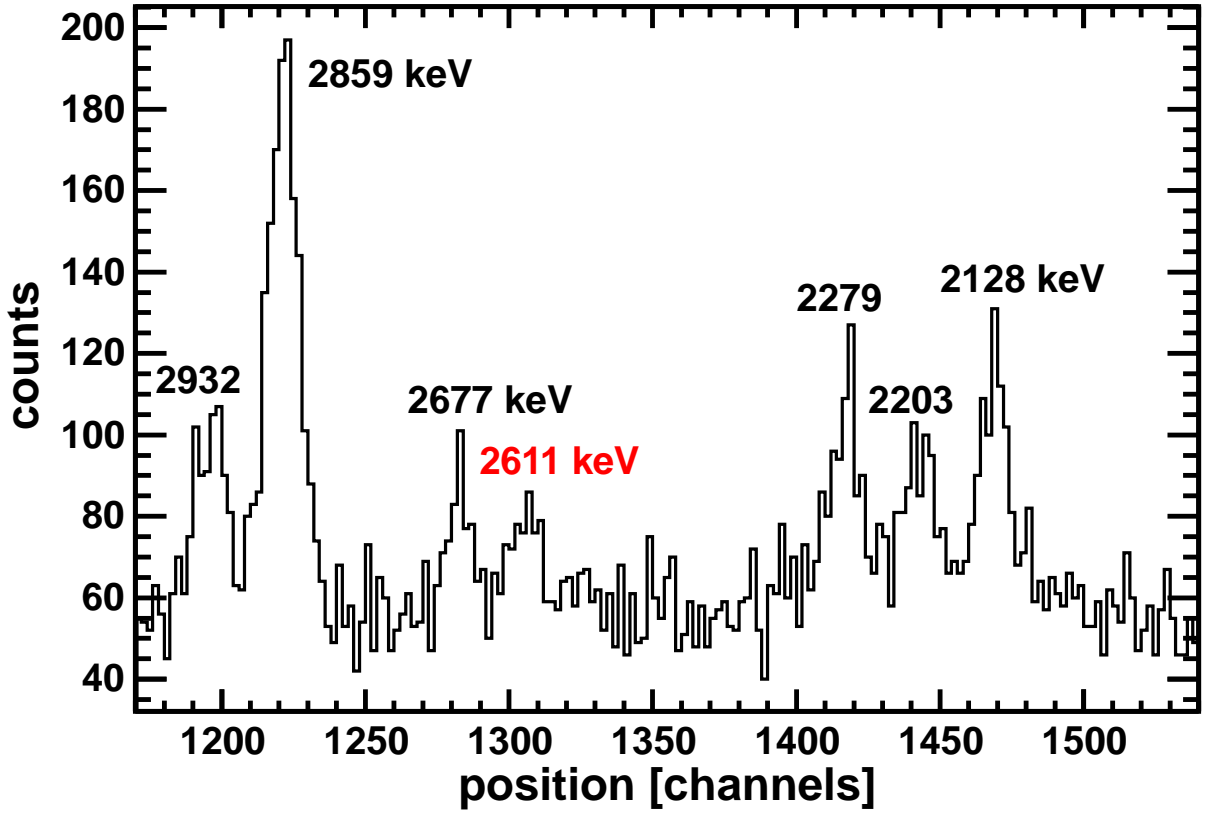
FIG. 2. (Color online) Focal-plane position spectrum with the Enge spectrograph set at $10°$ showing the newly discovered 2611 keV state in ^{32}Cl produced in the 350 μg/cm^2 ZnS target.

The events below the gated region in Fig. 3 corresponds to the proton decay of ^{16}F*, while events above are caused by leakage of deuterons into the triton window in the particle identification cut.

The angular probability distributions of the emitted protons for the ^{32}Cl states between 2.1 and 3.9 MeV are shown in Fig. 4. Two neighboring YLSA strips are coupled together to reduce scatter due to the low statistics. The values come from the ratios of the number of events in the t-p coincidence peaks to the total number of tritons populating a given state in ^{32}Cl, both with background subtracted. These numbers were then divided by the YLSA efficiency estimated via the use of a Monte Carlo model [10].

Angular correlations of isolated nuclear levels can be described by a linear combination of even terms of the Legendre polynomials, $P_{2k}\left[\cos(\theta_{c.m.})\right]$, of center-mass angle $\theta_{c.m.}$ up to two times the proton orbital angular momentum ℓ, i.e.

$$W(\theta) = \sum_{k=0}^{\ell} A_k P_{2k}\left[\cos(\theta_{c.m.})\right],\tag{3}$$

which is symmetric around $\theta_{c.m.} = 90°$. The minimum order of the Legendre polynomial needed to fit the data is defined by statistical significance testing with a p-value [19] required to be > 0.05, corresponding to $\chi^2 < 14.07$, 12.59,

and 11.07 for 7, 6, and 5 free parameters, respectively. This function was constrained to be positive at each point, and the integral over the full solid angle must be ≤ 1. The function was then integrated over the full solid angle to obtain a total proton-branching ratio, b_p, as

$$b_p = \int_{\theta=0}^{\pi} 2\pi sin(\theta)W(\theta)d\theta. \tag{4}$$

The results are shown in Table II with P_{fit} being the order of the Legendre polynomial used in the fit. The quoted proton branching-ratio uncertainties come from the uncertainties in the fit parameters.

The proton-branching ratio for the first excited state above the proton separation energy, $E_x = 1734.2$ keV, is expected to be small. However, even if it was a significant branch, the proton energy resulting from the $E_r = 153$ keV resonance is below the YLSA detector threshold, and would not be observed. The angular distributions of states
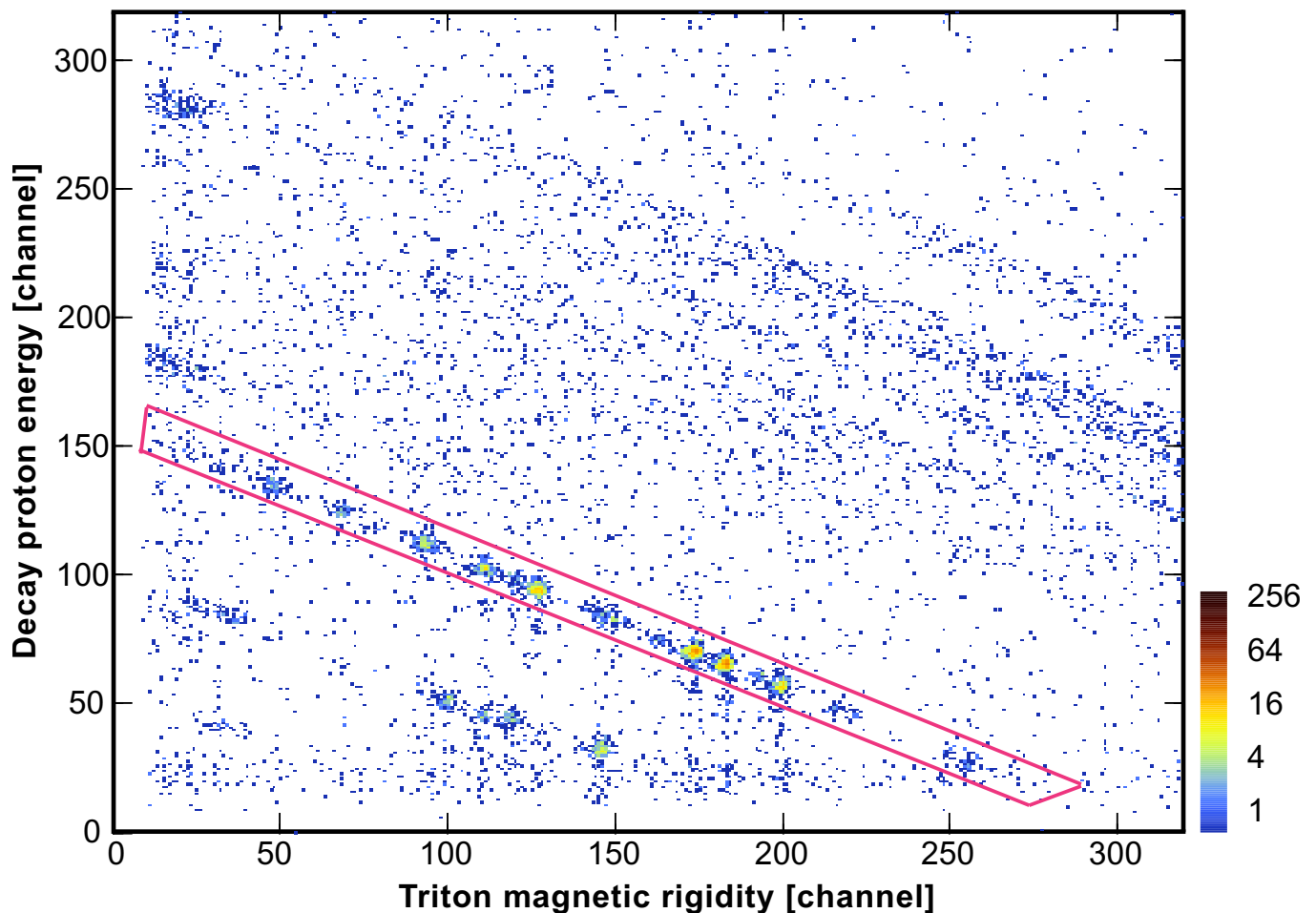

FIG. 3.   (Color online) Triton energy - proton energy coincidence spectrum.   The gated band corresponds to the ^{32}S(^{3}He,t)^{32}Cl*(p)^{31}S reaction.
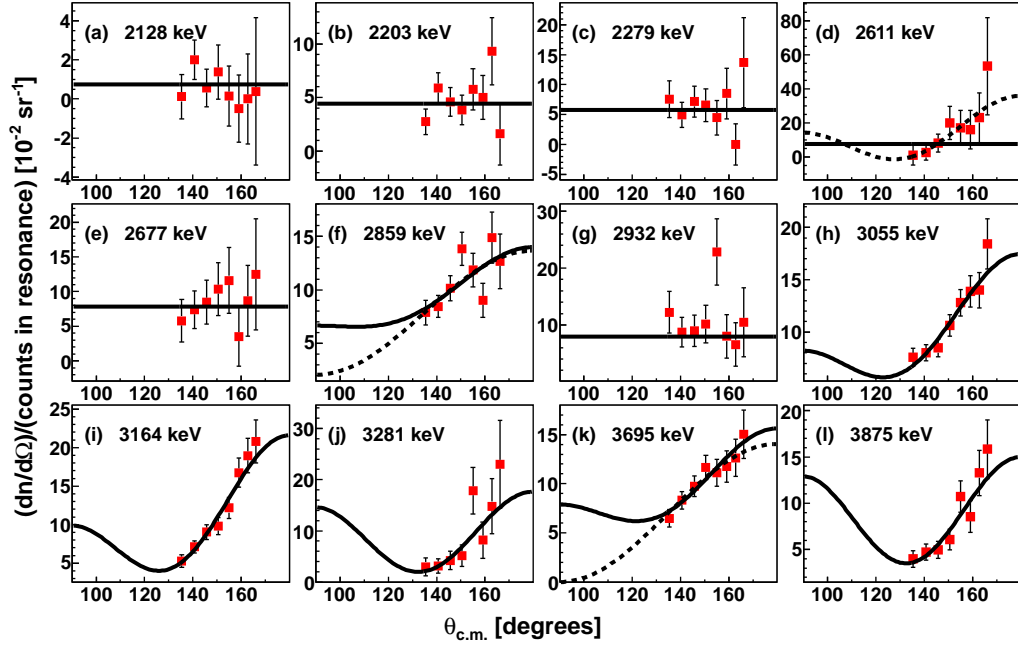
FIG. 4. (Color online) Triton-proton angular correlation probabilities from the ^{32}S(^{3}He,t)^{32}Cl(p)^{31}S reaction at 30 MeV for the various states in ^{32}Cl as listed in Table I. Red squares are the experimentally determined values with uncertainties, the black lines are the fits with even Legendre-polynomial terms. The polynomial orders are listed in Table II. Although the 2nd order Legendre polynomial (dashed line) for the 2859 keV and 3659 keV states describes the data well, we assume the 4th order Legendre polynomial to be correct (solid line).

with excitation energies of 2128 keV, 2203 keV, 2279 keV, 2611 keV, 2677 keV, and 2932 keV are well fit with just a constant function, requiring only the first term in Eq. 3.

The new state at 2611 keV presents an interesting case. Fits are shown in Fig. 4 using only an isotropic term (solid line) and the 4th order Legendre polynomial (dashed line). The angular distribution for this state is better fit with the 4th order Legendre polynomial, but the isotropic fit fulfills the p-value test [19] at the 95% confidence level and cannot be ruled out. As the excitation energy agrees well with that expected for a state corresponding to a 1^{+} state in the mirror [4], we adopt the 1^{+} assignment and use the isotropic angular distribution required from a ℓ=0 proton orbital angular momentum.

For the 2859 keV state, the 2nd order Legendre polynomial fulfills the p-value test giving a total proton-branching ratio of 75$\pm$5 %. However, a fit with the 4th order Legendre polynomial (dashed line in Fig. 4) differs from the previous one only outside the area covered with our data points, giving a total proton-branching ratio >95%. The neutron spectroscopic factor for the mirror state in ^{32}P has been measured to be 0.03 [22] and 0.008 [23]. While there

is a discrepancy between the measurements, even the lower value implies an expected proton width for the 2859 keV level that would be about 3 orders of magnitude larger than the expected gamma width. Therefore, we adopt the result from the 4th order Legendre polynomial fit.

The situation is similar for the 3695 keV state. We find a total proton-branching ratio of 59±4 % coming from the fit with the 2nd order Legendre polynomial and a branching ratio of >96% using a 4th order Legendre polynomial. While the mirror assignment is not as clear for the 3695 keV state, the most likely candidate, the 3880 keV (2^+), has a measured spectroscopic factor of 0.028 [22], in agreement with ≈0.03 predicted for the ^{32}Cl state by shell model calculations [24]. This is a factor of 15 more than the spectroscopic factor required for the branching ratio of 59% and we therefore adopt >96% from the 4th order Legendre polynomial fit.

For the 3055, 3164, 3281 and 3875 keV states, a 4th order Legendre polynomial fit is required, and the resulting branching ratio is consistent with $b_p = 100\%$. The lower limit for these states is then statistically estimated based on the number of events.

TABLE II. Proton-branching ratios for states in ^{32}Cl. Spin-parities assigned based on [4], except for 3695 keV and 3875 keV states that we assigned based on the mirror symmetry.

E_x [keV]	J^π	P_{fit}	b_p [%]
2128	3^+	0	7 ± 4
2203	1^+	0	54 ± 7
2279	2^+	0	66 ± 13
2611	1^+	0	$>62^a$
2677	2^+	0	$>78^b$
2859	3^+	4	>95
2932	2^-	0	>88
3055	4^-	4	>97
3164	3^-	4	>96
3281	2^+	4	>88
3695	2^+	4	>96
3875	3^+	4	>94

[a] Fit result is (95±32)%.
[b] Fit result is (94±16)%.

TABLE III. Properties of proton-unbound states in ^{32}Cl and corresponding resonances relevant for the ^{31}S$(p,\gamma)^{32}$Cl reaction. Energies (including systematic and statistical uncertainties) are the result from this work, except for 3767(10) keV from [16] and 3397(50) keV predicted by [4]. The spin-parity assignments from [4] were used for the states up to 3.5 MeV, from [16] for the 3767 keV state, for the 3695 and 3875 keV states were tentatively assigned based on the mirror symmetry.

E_x	E_r	J^π	Γ_γ	Γ_p	$\omega\gamma$	$\sigma(\omega\gamma)$
[keV]	[keV]		[meV]	[meV]	[meV]	[meV]
1734	153(5)	3^+	1.0	2.8×10^{-8}	4.9×10^{-8}	1.0×10^{-8} [a]
2128	546(5)	3^+	7.9	0.59	0.96	0.61
2203	622(5)	1^+	15.5	18.2	6.3	3.6
2279	697(5)	2^+	3.1	6.0	2.54	0.76
2611	1030(5)	1^+	20.2		14.4	7.5
2677	1096(5)	2^+	57.9		68	30
2859	1278(4)	3^+	5.4		9.5	3.7
2932	1350(5)	2^-	2.3		2.84	0.76
3055	1473(5)	4^-	0.8		1.81	0.42
3164	1583(4)	3^-	2		3.51	0.96
3281	1700(5)	2^+	15		18.3	8.5
3397	1816(50)	4^+	1.8		4.1	1.4
3695	2114(4)	2^+	28		35	20
3767	2186(10)	1^+	110		83	34
3875	2294(4)	3^+	59		104	65

[a] The uncertainty distribution of the 153 keV resonance strength includes an additional log-normal component with $\sigma_{log}(\omega\gamma) = 0.58$.

The obtained values for minimum proton orbital angular momenta are in a good agreement with assumed spins and parities. The spin-parity assignments for states with $E_x < 3.5$ MeV are taken from [4]. The spins of the 3695 and 3875 keV states were tentatively assigned based on the mirror symmetry corresponding to the 3880.3 keV 2^+ and 3989.8 keV (3^+) states in ^{32}P [15], as the 3796.1 keV (1^+) in ^{32}P is assumed to be the mirror state to the 3767 keV state in ^{32}Cl that is known to be $J^\pi = 1^+$ [16].

V. ^{31}S(p,γ)^{32}Cl REACTION RATE

At nova temperatures, $T \approx 0.1$–0.3 GK, the states just above the proton-separation energy ($Q_p = 1581.3$ keV) dominate the ^{31}S(p,γ)^{32}Cl reaction rate. As the resonances are generally narrow and well separated, the resonant component of the reaction rate (in cm^{3}mol^{-1}s^{-1}) can be approximated by

$$N_A\langle\sigma v\rangle = 1.54 \times 10^{11}(\mu T_9)^{-3/2}$$

$$\times \sum_r (\omega\gamma)_r \exp(-11.605 E_r/T_9), \tag{5}$$

where T_9 is the temperature in GK, E_r is the energy of the ^{32}Cl resonance in MeV, μ is the reduced mass in atomic mass units, and $(\omega\gamma)_r$ is the resonance strength in MeV, given by the spin of the resonance, J_r and its partial (Γ_p,Γ_γ) and total (Γ) widths as

$$(\omega\gamma)_r = \frac{(2J_r + 1)}{4}\frac{\Gamma_p\Gamma_\gamma}{\Gamma}. \tag{6}$$

The resonance reaction rate depends exponentially on the resonance energies, E_r, and linearly on the partial widths through the resonance strengths, though the proton partial width, Γ_p, also has an exponential dependence on energy through the penetrability. Therefore, our improved measurement of the resonance energies and the proton-branching ratios, corresponding to $\Gamma_p/\Gamma = \Gamma_p/(\Gamma_p + \Gamma_\gamma)$, has a direct impact on the uncertainty in the ^{31}S(p,γ)^{32}Cl reaction rate.

We have calculated the gamma widths for the states in ^{32}Cl using the known half-lives of mirror ^{32}P states, $T_{1/2}$, as well as γ-branching ratios, b_γ, and energies, E_{γ_i}, of the corresponding transitions from the states [20]. Assuming that the reduced transition probabilities, $B(E_i)$ and $B(M_i)$, are the same for both mirror nuclei, one can calculate the γ width of a state in the mirror nucleus as a sum through all possible final state transitions:

$$\Gamma_\gamma\left(^{32}\text{Cl}\right) = \sum_i \frac{E_{\gamma_i}^{(\lambda_i+2)}(^{32}\text{Cl})}{E_{\gamma_i}^{(\lambda_i+2)}(^{32}\text{P})}\frac{b_\gamma\hbar\ln(2)}{T_{1/2}(^{32}\text{P})}, \tag{7}$$

where λ is electric or magnetic multipolarity. This follows a similar prescription as was used in [4, 5]. The lowest possible multipolarities were assumed. In the case of $M1/E2$ transitions, studies of the mirror nucleus [20] showed that $M1$ transitions mostly dominate, and thus $M1$ transitions were adopted in the present reaction rate calculations.

For the excited states between 2.1 MeV and 2.3 MeV, where the proton-branching ratio was determined to be finite but less than 100%, we calculated the proton widths, Γ_p, directly from the gamma widths with our measured proton-branching ratios. For the higher energies, the resonance strength becomes insensitive to the proton width as $\Gamma_p \gg \Gamma_\gamma$ and $\Gamma_p\Gamma_\gamma/\Gamma \sim \Gamma_\gamma$.

The 1734 keV state, corresponding to the 153 keV resonance, is the one state where the proton decay width is important, but where no information was extracted from our measurement. In this case we calculated the proton width using the prescription also followed in [4],

$$\Gamma_p = 2\frac{\hbar^2}{\mu a_c^2}P_c C^2 S_p \theta_{sp}^2,\tag{8}$$

where μ is the reduced mass and $a_c = 5.6$ fm is the channel radius. The single-particle reduced width, $\theta_{sp}^2 = 0.32$, was derived from the parameterization for nuclei with the mass number $A = 12$–50 and bombarding energies $E \leq 1000$ keV based on optical-model computations and R-matrix expressions [21]. The penetrability was calculated to be $P_c = 2.9 \times 10^{-15}$. The spectroscopic factor, $C^2 S_p$, was obtained from the reaction studies with the mirror nucleus ^{32}P produced via a neutron transfer, ^{31}P$(d,p)^{32}$P, at deuteron energies of 10 MeV [22] and 20 MeV [23]. The spectroscopic factors reported in these measurements are discrepant, 0.011 [22] and 0.0054 [23], and the average value was adopted in [4, 5]. However, we conducted a reanalysis of the experimental cross section data from [22] and [23] using the FRESCO code [25]. We find differential cross-sections from both experiments to be best fit with a spectroscopic factor of 0.011, in agreement with [22]. Thus, we adopt the higher value for the spectroscopic factor and from this calculate the proton width of the 153(5) keV resonance to be 2.8×10^{-8} meV.

The calculated proton and gamma widths, as well as resonance strengths calculated using Eq. 6, are listed in Table III. The resonance energies determined in this work have been used for the calculations, except for the 3767 keV state measured in the ^{32}Ar β-decay studies [16] and the 3397 keV state predicted by [4] based on the mirror symmetry.

To cover temperatures below the regions dominated by the resonances, we have adopted the direct capture parameterization from [4]. The recommended total ^{31}S$(p,\gamma)^{32}$Cl reaction rate for the stellar temperature range $T = 0.01$–10 GK is given in Table IV. The individual contributions of direct and resonant capture are illustrated in Fig. 5. The rate has been parameterized in the Reaclib format [26] as the sum of three exponentials, each with a set of 7 parameters in the form

$$N_A\langle\sigma v\rangle = \exp\left[a_0 + a_1/T_9 + a_2/T_9^{1/3} + a_3 T_9^{1/3}\right.$$
$$\left.+ a_4 T_9 + a_5 T_9^{5/3} + a_6 \times \ln(T_9)\right]\tag{9}$$

where T_9 is the temperature in GK, using the tools in [27]. The fit agrees with the data within 1.5%. The new Reaclib parameters are listed in Table V.

Uncertainties in the reaction rate have been estimated using a Monte Carlo technique, as a combination of normal
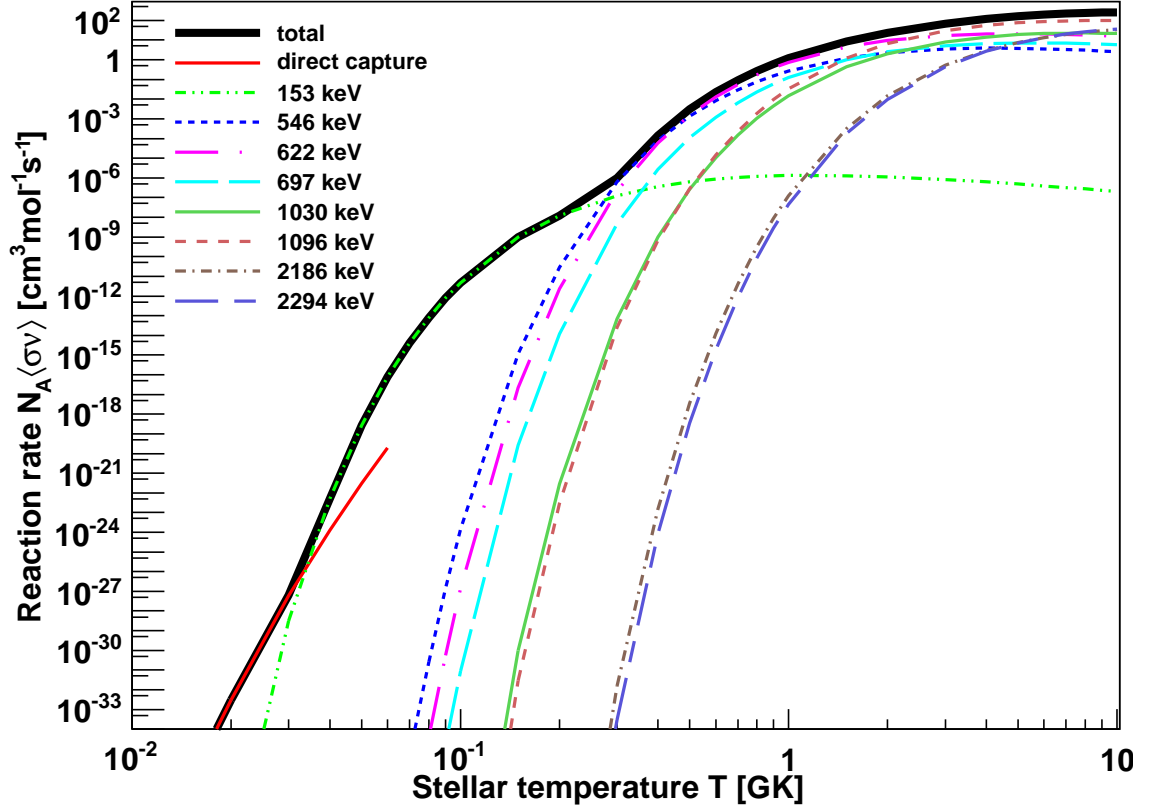
FIG. 5. (Color online) ^{31}S$(p,\gamma)^{32}$Cl reaction rate as a function of the stellar temperature T. Resonances with a contribution of at least 10% contribution are shown.

and log-normal distributions of uncertainties complicate the analysis. Uncertainties in the resonance energies contribute to the log-normal distribution, as the energy is in the exponential of Eq. 5. The gamma width contributes to the normal distribution, as its uncertainty originated from the half-life uncertainty, mirror-symmetry assumption (that we have estimated to be 20% based on the mirror states in the neighboring nuclei) and the uncertainty of the proton-branching ratio. The uncertainty in the proton width will have a pure normal distribution, if extracted from the proton-branching ratio. For the 153 keV resonance, the exponential dependence of the penetrability on the energy contributes to the log-normal distribution, but a normally distributed contribution also originates in the spectroscopic factor uncertainty that we have estimated to be 30%, the spectroscopic factor being different for both mirror nuclei due to the effect of Coulomb and other isospin-nonconserving interactions ($\sim$10%), a small uncertainty of the wavelength in the penetrability ($\sim$2%), and the reduced width uncertainty that we have estimated to be 20%. For the 3695 keV and 3875 keV states, the uncertainty in the spins is considered. Estimated uncertainties for the resonance strengths are shown in Table III. Direct capture uncertainties were taken directly from [5].
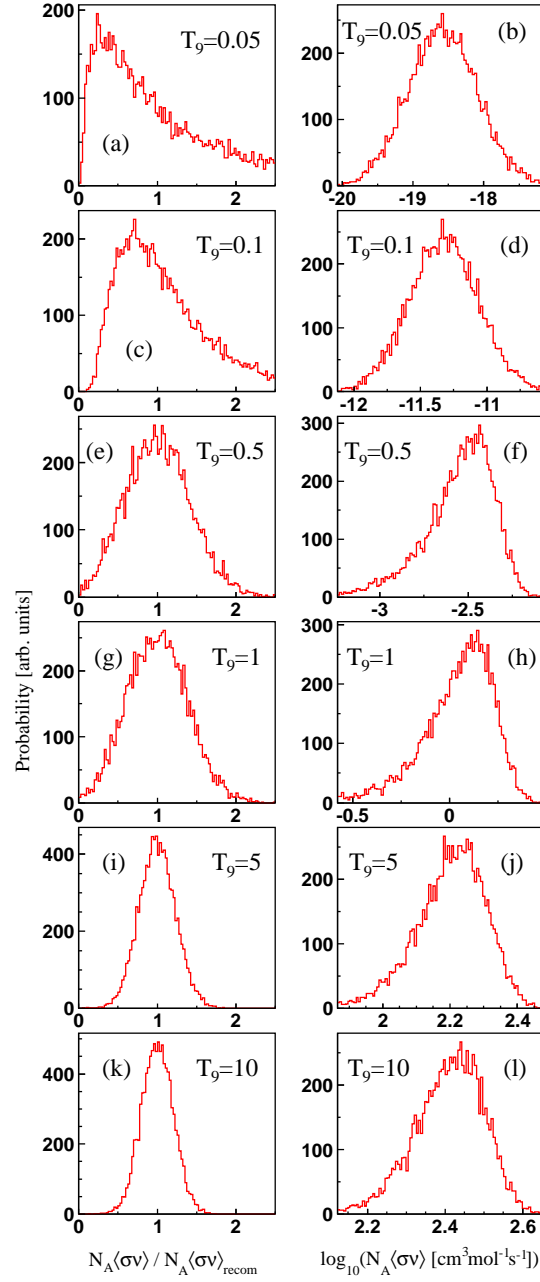
FIG. 6. (Color online) Total reaction rate probability density functions as a result of the Monte Carlo simulation of the input-uncertainty propagation for various temperatures. The left figures show the distributions in the logarithmic scale normalized to the recommended value, the right figures show the same distributions in logarithmic scale without normalization.

In the simulation, the values of the energies and resonance strengths were varied randomly as a Gaussian distribution. Correlations, when dependent on the same parameters, were taken into account. The resulting reaction rate distributions (see Fig. 6) have various shapes for different temperatures, including a nearly pure log-normal distribution at $T = 0.05$ GK and normal distribution at $T = 5$ GK. To give final uncertainties that would correspond to the

standard deviation σ in both distributions, we found a lower limit as a value with a percentile of 15.9 and an upper limit with a percentile of 84.1, covering the 68.2% confidence level. The results from the Monte Carlo simulation are listed as the low and high rates in Table IV.

VI.   DISCUSSION

The total ^{31}S$(p,\gamma)^{32}$Cl reaction rate and individual contributions based upon this work are illustrated in Fig. 5. Direct capture dominates the reaction rate up to $T \sim 0.03$ GK. The 153 keV, 546 keV, 622 keV, and 1096 keV resonances, corresponding to 1734 keV, 2128 keV, 2203 keV, and 2677 keV levels in ^{32}Cl, dominate the rate over nearly all temperatures. The 697 keV resonance contributes more than 10% at nova temperatures, and the 1030 keV resonance must be considered at X-ray burst temperatures, $T \approx 2$ GK. The 2186 keV, and 2294 keV resonances do not contribute except at very high temperatures, $T > 5$ GK, and the 2859 keV and 3695 keV levels (which had some ambiguity as to the shape of the proton angular distribution) make a negligible contribution to the reaction rate.

The ^{31}S$(p,\gamma)^{32}$Cl reaction rate with uncertainties was recently calculated by [5] using the previous work of [4] with the evaluated level energies from [15]. The ratio of the rate from Ref. [5] to our rate is shown in Fig. 7. The uncertainties in both rates are illustrated by the hashed regions. The agreement for $T < 0.03$ GK is expected, as the direct capture rate was calculated based on the same parameters [4], and the lower and upper limits we take from [5].

Over much of the range of nova temperatures our recommended rate is significantly greater than even the "high rate" recommended in Ref. [5]. This arises from the contribution of individual resonances. In Fig. 8 the individual resonance reaction rates from Ref. [5] are compared to our results. Our higher reaction rate at most nova temperatures arises from the fact that the resonance energies adopted in Ref. [4] (and derived from [15]) are greater than our energies by 6-15 keV (9 keV on average). The excitation energies adopted by [15] and [4] primarily reflect a weighted average of [3] and [7] after the results of [7] were shifted to match the 1168 keV excitation energy. The 3-5 keV uncertainties in the adopted excitation energies do not properly reflect systematic uncertainties, such as uncertainties in the calibration used or the discrepancies between measurements.

Our rate also differs from that of [5] due to improved values for resonance strengths. It should be noted that while we adopt a resonance strength for the 153 keV resonance that is nearly the same as [4, 5], this arises from two significant changes that largely cancel each other. Our lower resonance energy results in a significantly smaller penetrability, but we recommend a significantly greater spectroscopic factor based on our reanalysis of the transfer
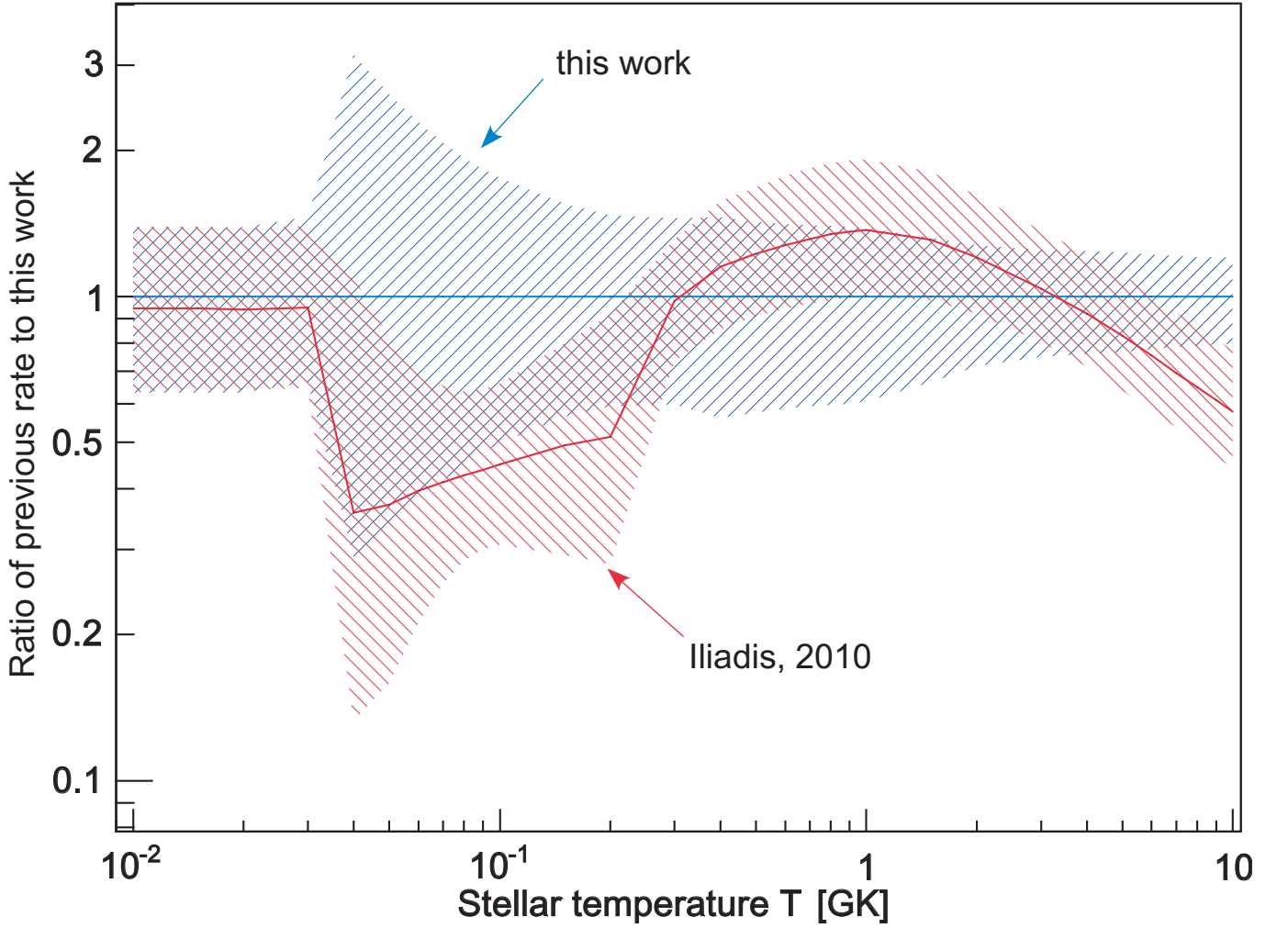
FIG. 7. (Color online) The ^{31}S$(p,\gamma)^{32}$Cl reaction rate with uncertainties calculated by [5] (red), with only statistical uncertainties considered, is compared to the results from this work (blue), with both statistical and systematic uncertainties considered. Values are shown normalized to the recommended rate from this work.

data of [22, 23]. Our reaction rate near peak nova temperatures, $T \approx 0.3$ GK, becomes smaller than that of [5] due to our improved values for the proton branching ratios of the 546 and 622 keV resonances. We find Γ_p for the 546 keV resonance to be about 30% smaller than estimated by [4] and Γ_p for the 622 keV resonance to be about 2 orders of magnitude smaller. The smaller proton widths result in smaller resonance strengths and reaction rates, though the magnitude of the effect is mitigated by the lower value of the resonance energies for these states that makes for a smaller decrease in the reaction rate than would otherwise be.

At higher temperatures (above about 2 GK) our rate increases in comparison to [4] due to our inclusion of resonances above 2 MeV that were not previously considered.
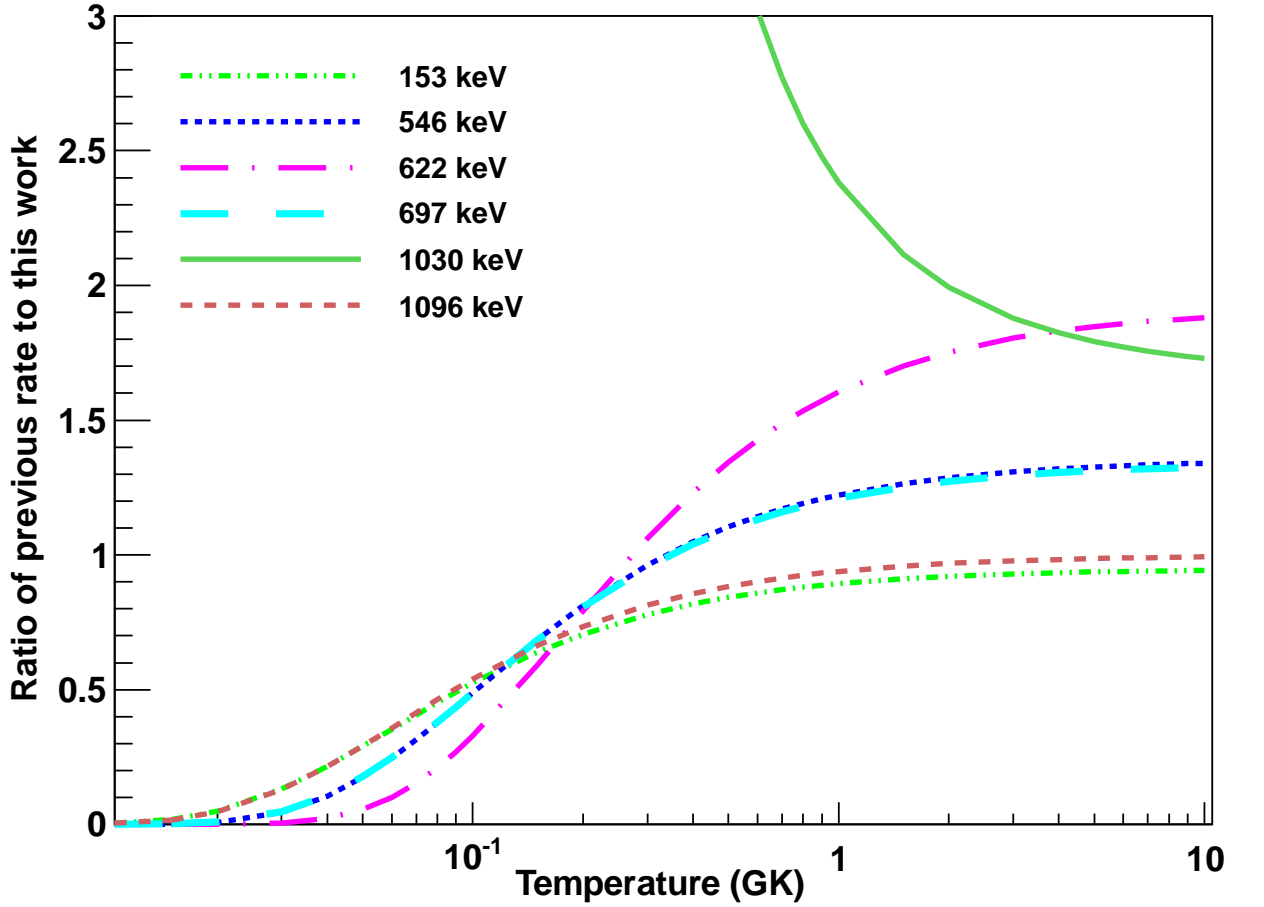
FIG. 8. (Color online) The ratio of the individual resonance reaction rates from Ref. [5] to rates from this work as a function of stellar temperature for the most important resonances contributing to the ^{31}S$(p,\gamma)^{32}$Cl rate.

In summary, we have significantly improved the resonance energies and resonance strengths for some of the most important resonances in the ^{31}S$(p,\gamma)^{32}$Cl reaction. An important aspect of the current work is that we have given careful consideration to uncertainties, including systematic uncertainties in the level energies, states used for calibration, and target thickness effects. The largest uncertainties in the reaction rate at nova temperatures arise from the systematic uncertainty in the resonance energies and the resonance strength of the 153 keV resonance. Our excitation energy for the 1734.2(14) keV state (corresponding to the 153 keV resonance) differs from the value of 1736.7(6) reported by [8] (which used a slightly different set of calibration reactions) by 2.5 keV or slightly more than 1σ. However, we estimate the systematic uncertainty in the resonance energies to be 4 keV, which is in agreement with the fact that the excitation energies for all levels reported by [8] are higher on average than this work by about 4 keV. Additional experimental information leading to an improvement in the resonance energies would therefore be valuable. As the states most important for novae have substantial branches for gamma decay, an accurate measure-

ment of gamma-ray energies using a complementary approach, for example as in [28], would be particularly helpful in reducing the systematic uncertainties that arise largely from Q-value uncertainties in reaction studies like this one. A direct measurement of the resonance strength of the 153 keV resonance (or corresponding proton width) is also desired, but would be experimentally challenging.

[1] R. E. Williams, M. M. Philipps, and M. Hamuy, Astrophys. J. Suppl. Ser. **90**, 297 (1994).

[2] T. Matheson, A. V. Filippenko, and L. C. Ho, Astrophys. J. **418**, L29 (1993).

[3] S. Vouzoukas *et al.*, Phys. Rev. C **50**, 1185 (1994).

[4] C. Iliadis, P. M. Endt, N. Prantzos, and W. J. Thompson, Astrophys. J. **524**, 434 (1999).

[5] C. Iliadis, R. Longland, A.E. Champagne, A. Coc, and R. Fitzgerald, Nucl. Phys. **A841**, 31 (2010).

[6] M. Bhattacharya, *et al.*, Phys. Rev. C **77**, 065503 (2008).

[7] C. Jeanperrin, L. H. Rosier, B. Ramstein, and E. I. Obiajunwa, Nucl. Phys. **A503**, 77 (1989).

[8] C. Wrede *et al.*, Phys. Rev. C **82**, 035805 (2010).

[9] A. Parikh, Ph.D. thesis, Yale University (2006).

[10] D. W. Visser, Ph.D. thesis, Yale University (2003).

[11] G. Audi, O. Bersillon, J. Blachot, and A. H. Wapstra, Nucl. Phys. **A729**, 3 (2003).

[12] www.nuclearmasses.org.

[13] C. Wrede *et al.*, Phys. Rev. C **81**, 055503 (2010).

[14] K. Braune, R. Novotny, D. Pelte, D. Husar, and D. Schwalm, Proc. German Phys. Soc. 4 (1978).

[15] P. M. Endt, Nucl. Phys. **A633**, 1 (1998).

[16] T. Björnstad *et al.*, Nucl. Phys. **A443**, 283 (1985).

[17] D. Schardt, and K. Riisager, Z. Phys. **A345**, 265 (1993).

[18] P. M. Endt, Nucl. Phys. **A521**, 1 (1990).

[19] R. E. Walpole, R. H. Myers, S.L. Myers, and K. Ye, Probability and Statistics for Engineers and Scientists (7th ed.), New York: Macmillan (2002).

[20] A. Kangasmäki, P. Tikkanen, J. Keinonen, W. E. Ormand, and S. Raman, Phys. Rev. C **55**, 1697 (1997).

[21] C. Iliadis, Nucl. Phys. **A618**, 166 (1997).

[22] J. J. M. van Gasteren, A. J. L. Verhage, and J. F. van der Veen, Nucl. Phys. **A210**, 29 (1973).

[23] F. J. Eckle, G. Eckle, F. Merz, H. J. Maier, H. Kader, and G. Graw, Nucl. Phys. **A501**, 413 (1989).

[24] B. A. Brown (private communication).

[25] I. J. Thompson, Comput. Phys. Rep. **7**, 167 (1988).

[26] F.-K. Thielemann, M. Arnould, and J. W. Truran, in Adv. Nucl. Astrophys., ed. E. Vangioni-Flam, J. Audouze, M. Cass, J.-P. Chieze, & J. Tran Thahn Van, 525 (1987).

[27] www.nucastro.org.

[28] D. Seweryniak *et al.*, Phys. Rev. C **75**, 062801 (2007).

TABLE IV. Recommended stellar reaction rates as a function of the temperature T for the reaction ^{31}S$(p,\gamma)^{32}$Cl. Lower and upper limits cover the 68.2% confidence level.

Tempe-rature T [GK]	Recommended rate $N_A\langle\sigma v\rangle$ [cm^{3}mol^{-1}s^{-1}]	Low rate $N_A\langle\sigma v\rangle$ [cm^{3}mol^{-1}s^{-1}]	High rate $N_A\langle\sigma v\rangle$ [cm^{3}mol^{-1}s^{-1}]
0.01	3.68×10^{-44}	2.33×10^{-44}	5.12×10^{-44}
0.015	1.84×10^{-37}	1.17×10^{-37}	2.56×10^{-37}
0.02	3.08×10^{-33}	1.95×10^{-33}	4.28×10^{-33}
0.03	6.33×10^{-28}	4.36×10^{-28}	1.02×10^{-27}
0.04	5.39×10^{-23}	1.39×10^{-23}	2.12×10^{-22}
0.05	2.69×10^{-19}	8.50×10^{-20}	8.10×10^{-19}
0.06	7.56×10^{-17}	2.86×10^{-17}	1.91×10^{-16}
0.07	4.10×10^{-15}	1.76×10^{-15}	9.13×10^{-15}
0.08	7.98×10^{-14}	3.77×10^{-14}	1.62×10^{-13}
0.09	7.86×10^{-13}	4.00×10^{-13}	1.48×10^{-12}
0.1	4.82×10^{-12}	2.59×10^{-12}	8.61×10^{-12}
0.15	9.73×10^{-10}	6.17×10^{-10}	1.48×10^{-9}
0.2	1.22×10^{-8}	8.42×10^{-9}	1.71×10^{-8}
0.3	9.86×10^{-7}	5.70×10^{-7}	1.45×10^{-6}
0.4	1.41×10^{-4}	7.90×10^{-5}	2.05×10^{-4}
0.5	2.99×10^{-3}	1.73×10^{-3}	4.26×10^{-3}
0.6	2.27×10^{-2}	1.33×10^{-2}	3.20×10^{-2}
0.7	9.47×10^{-2}	5.61×10^{-2}	1.33×10^{-1}
0.8	2.73×10^{-1}	1.63×10^{-1}	3.81×10^{-1}
0.9	6.17×10^{-1}	3.70×10^{-1}	8.59×10^{-1}
1	1.18×10^{0}	7.16×10^{-1}	1.63×10^{0}
1.5	8.39×10^{0}	5.59×10^{0}	1.11×10^{1}
2	2.37×10^{1}	1.69×10^{1}	3.01×10^{1}
3	6.99×10^{1}	5.25×10^{1}	8.71×10^{1}
4	1.20×10^{2}	9.08×10^{1}	1.48×10^{2}
5	1.63×10^{2}	1.25×10^{2}	2.00×10^{2}
6	1.97×10^{2}	1.53×10^{2}	2.41×10^{2}
7	2.23×10^{2}	1.75×10^{2}	2.70×10^{2}
8	2.41×10^{2}	1.91×10^{2}	2.91×10^{2}
9	2.53×10^{2}	2.02×10^{2}	3.06×10^{2}
10	2.61×10^{2}	2.08×10^{2}	3.14×10^{2}

TABLE V. Recommended Reaclib parameters for the ^{31}S$(p,\gamma)^{32}$Cl reaction rate within $T = 0.01$–10 GK.

set	a_0	a_1	a_2	a_3	a_4	a_5	a_6
1	297.13	-2.6702	114.07	-485.67	63.95	-5.699	140.32
2	-35.362	4.1263	-324.5	373.08	-18.087	0.9159	-205.99
3	1315.5	-1.8787	330.21	-1911.9	261.17	-25.381	511.02